JOURNAL OF AGRICULTURAL AND FOOD CHEMISTRY

ARTICLE

pubs.acs.org/JAFC

Using High Intensity Ultrasound as a Tool To Change the Functional Properties of Interesterified Soybean Oil

Yubin Ye, Ashwini Wagh, and Silvana Martini*

Department of Nutrition, Dietetics, and Food Sciences, Utah State University, 8700 Old Main Hill, Logan, Utah, 84322-8700

ABSTRACT: High intensity ultrasound (HIU) was used to change the crystallization behavior, generate small crystals, and improve the texture of a low saturated shortening (interesterified soybean oil). Samples were crystallized at different temperatures (26, 28, 30, and 32 °C) without and with the application of HIU. Different acoustic power levels (110, 72, 61, 54, and 44 W) were used. Results show that higher acoustic powers had a greater effect on crystal size reduction, induced crystallization, and generated harder, more elastic and viscous materials. These effects were more significant when HIU was applied in the presence of crystals and when the sample was crystallized at 32 °C.

KEYWORDS: High intensity ultrasound, crystallization, interesterified soybean oil, rheology, hardness, morphology

INTRODUCTION

The Institute of Shortening and Edible Oils reports an 85% increase in the consumption of shortenings in the last 10 years.[1] During this period, the food industry has gradually replaced the use of animal fat with modified vegetable oils. Even though vegetable oils have been used for decades, the lack of texture and plasticity of some vegetable oils have limited their use in food products. To overcome this limitation, different processing technologies, together with new varieties of vegetable oils, have been developed to provide shortenings with a wide range of functional properties that can be used by food producers. During the early stages of shortening production, partial hydrogenation was used to improve the functional properties of vegetable oils. Depending on the degree of hydrogenation, shortenings with different solid/liquid ratios can be obtained in an easy and economical manner that can be used for specific applications in the food industry. However, research has shown a strong correlation between *trans*-isomers generated by the hydrogenation process and the incidence of coronary heart disease.[2−8] This finding, together with the trend of adopting healthier lifestyles, has encouraged food manufacturers to produce food products with little or zero *trans*-fatty acid content. In addition, since 2006, the FDA has required declaration of *trans*-fatty acid content on food labels, with 0.5 g of *trans*-fatty acid per serving to be labeled as "no *trans*-fat" [21 CFR 101.9(C)(2)-(ii)]. Interesterified oils,[9−13] semisolid oils such as palm and coconut, and lipid blends have been used to replace *trans*-fats in food formulations. The use of low saturated shortenings in food formulations is one potential solution to replace *trans*-fats; however, these shortenings are usually too soft for some food applications, leading to low functionality and quality of products.[14] To find a balance between nutritional and functional properties, different processing conditions can be used to improve the physicochemical characteristics and functionality of shortenings and meet consumers' expectations.[15]

High intensity ultrasound (HIU) has been used in the food industry as an efficient tool for large scale commercial applications, such as emulsification, homogenization, extraction, crystallization, and viscosity alteration.[16] There is a myriad of literature describing the use of HIU to induce or generate crystallization (sonocrystallization) in aqueous systems. To name a few studies performed in the food science area, Dr. Malcom Povey's group described the use of ultrasonic crystallization to control the size and rate of ice crystals formation in frozen foods.[17] In addition, this same researcher further proved that HIU can modify the primary and secondary nucleation of ice,[18] while Patel et al.[19] showed that the use of power ultrasound can control the crystallization process of lactose during the nucleation phase. In 2007, McCausland showed that HIU can be used to produce crystalline materials for pharmaceutical uses.[20] In general, previous research has shown that HIU can affect crystallization processes by either affecting crystal nucleation, controlling the rate of crystal growth, promoting the formation of small and even-sized crystals, and preventing fouling of surfaces by the newly formed crystals.[21−23] Early work by Sato's group in lipid systems has shown that HIU induced the crystallization of tripalmitin and cocoa butter and also promoted the formation of β' and β crystals.[24−26] Previous research in our laboratory has shown that HIU can induce the crystallization of other fats such as anhydrous milk fat,[27] palm kernel oil, and an all-purpose shortening.[28] The literature provides significant information on the effect of HIU on the crystallization behavior of different molecules in aqueous systems; however, there is very little information on the effect of HIU on the crystallization kinetics, polymorphism, and rheological behavior of lipids, shortenings in particular.

The objective of this work was to evaluate the effect of HIU on the crystallization behavior and functional properties of a low saturated shortening (interesterified soybean oil). Different sonication and processing conditions were tested, and the functional properties of the material, such as crystallization behavior, microstructure, melting profile, texture, viscoelasticity, and polymorphism, were measured.

Received: June 22, 2011
Accepted: September 6, 2011
Revised: September 5, 2011
Published: September 06, 2011

dx.doi.org/10.1021/jf202495b | *J. Agric. Food Chem.* 2011, 59, 10712–10722

Table 1. HIU Conditions and Nomenclature Used To Evaluate the Effect of HIU on the Crystallization Behavior and Functional Properties of Interesterified Soybean Oil (IESBO)

nomenclature	HIU condition
10/wo	sample reached T_c at 10 min (agitation stopped); no HIU is applied
10/10	sample reached T_c at 10 min (agitation stopped); HIU is applied at 10 min
10/13	sample reached T_c at 10 min (agitation stopped); HIU is applied at 13 min
10/20	sample reached T_c at 10 min (agitation stopped); HIU is applied at 20 min
5/wo	sample reached T_c at 5 min (agitation stopped); no HIU is applied
5/5	sample reached T_c at 5 min (agitation stopped); HIU is applied at 5 min

MATERIALS AND METHODS

Materials. A low saturated fat shortening consisting of interesterified soybean oil (IESBO) was used in this research. The shortening (product no. 76-240-0) was provided by Archer-Daniels-Midland (Decatur, IL) and produced by interesterification of liquid soybean oil and a fully hydrogenated hard stock. The chemical composition of the IESBO is described in the Results and Discussion.

Melting Point Determination. The melting point of IESBO was determined by AOCS official Method Cc 1−25.

Triacylglycerol (TAG) Chemical Composition. The TAG chemical composition was determined using AOCS official Method Ce 5b-89. The composition was expressed as the percentage of equivalent carbon number (ECN) molecular entities as described in the Materials and Methods.

Fatty Acid Methyl Esters (FAMEs) Chemical Composition. FAMEs of all samples were analyzed by gas chromatography on a Shimadzu 2010 GC equipped with a flame ionization detector (Shimadzu, Columbia, MD). FAMEs were prepared as described by O'Fallon et al. with slight modifications.[29] Samples were melted at 60 °C for 15 min; 40 μL of melted oil sample was then placed into a 16 mm × 125 mm screw-cap Pyrex culture tube to which 6.3 mL of MeOH and 0.7 mL of 10 N KOH in water were added. After the mixture was vortex-mixed, the tube was then incubated in a 55 °C water bath for 1.5 h with autoshaking to properly permeate, dissolve, and hydrolyze the sample. After the samples were cooled down to lower temperature in a bucket with ice water, 0.58 mL of 24 N H_2SO_4 was added. The tube was vortex-mixed and incubated in a water bath at 55 °C with autoshaking for 1.5 h. Two milliliters of hexane was added, and the tube was vortex-mixed before being centrifuged for 10 min at 1000*g* in a tabletop centrifuge. The hexane layer (upper phase), which contains the FAME, was placed into a GC vial, and the vial was capped and placed at −20 °C until GC analysis.

FAMEs were separated using a DB-225 fused-silica capillary column (20 m × 0.18 mm i.d. × 0.2 μm film thickness, Agilent Technologies, Palo Alto, CA). The injection was done in the split mode. One microliter was introduced into the injector at 250 °C, with a split ratio of 30:1. The carrier gas was hydrogen at a linear velocity of 61.2 cm/s. The oven temperature program was as follows: 35 °C held for 0.38 min, 33.21 °C/min to 195 °C, 3.99 °C/min to 205 °C, and 10.63 °C/min to 230 °C followed by a 5 min hold. The detector temperature was 250 °C with an air flow of 400 mL/min and hydrogen flow at 39 mL/min. Peaks were identified by retention time overlay with authentic FAME standards (Nu-Chek Prep, Elysian, MN).

Crystallization and HIU Application. IESBO was heated to 80 °C and kept at this temperature for 30 min to allow complete melting of the TAGs. The melted lipid sample was then placed in a thermostatized crystallization cell as described elsewhere,[27,28] which was set at different crystallization temperatures (T_c = 26, 28, 30, and 32 °C). IESBO was crystallized at a cooling rate of 5 °C/min with agitation using a magnetic stirrer (200 rpm) to increase the heat transfer between the sample and the external circulating water. Different crystallization experiments were performed during this research. The first set of experiments was performed to establish the acoustic power needed to achieve a greater effect in crystal size reduction during crystallization. For these sets of experiments, HIU was applied after 10 min into the crystallization experiments, which corresponded to the moment when the sample reached crystallization temperature. Before HIU was applied, agitation was stopped to avoid dissolution of bubbles generated during the sonication process. HIU was applied for 10 s (Misonix S-3000 sonicator, Misonix Inc., NY) using different acoustic power (110, 72, 61, 54, and 44 W). The sonicator operates at an acoustic frequency of 20 kHz, and a microtip of 3.2 mm diameter was used. After sonication, the sample was kept at a crystallization temperature for 90 min to allow complete crystallization. This was demonstrated by the lack of crystal change as observed in the polarized light microscope. The second set of experiments consisted of applying HIU using 110 W of acoustic power for 10 s. HIU was applied at different time points during the crystallization process as can be seen in Table 1. Crystal formation and morphology during crystallization were evaluated using polarized light microscopy. After the sample was held in the crystallization cell for 90 min, the functional properties of the shortenings were measured using the techniques described below. In addition, functional properties were measured after tempering the samples for 48 h at 5 and 25 °C. Samples crystallized without HIU application were used as control groups.

Polarized Light Microscopy Measurements (PLM). The crystal morphology was recorded during crystallization. A drop of lipid sample was taken from the crystallization cell at different times and placed between a slide and a cover-slide to evaluate crystals' microstructure during crystallization using a polarized light microscope (PLM, Olympus CX 31, Tokyo, Japan) with a digital camera attached. A total 200× magnification was used.

Thermal Behavior Measurements. A differential scanning calorimeter (DSC, DSC 2910, TA Instrument, United States) was used to evaluate the melting behavior of the crystallized material. After 90 min in the crystallization cell, 5−15 mg of sample was placed in a hermetic aluminum pan for DSC use. The sample was heated to 80 °C with a ramp rate of 5 °C/min to evaluate the melting behavior of crystallized material. Through this procedure, the melting enthalpy (ΔH) was determined. This evaluation provided information about the amount of solids generated during crystallization. The melting profile of the samples was quantified by integrating the melting endotherms at specific temperatures, and the percentage of solid fat at different temperatures during melting was calculated. Melting profiles and melting enthalpy values were also determined for samples tempered at 5 °C for 48 h.

Texture Profile Analysis. The hardness of the lipid network formed was measured by texture profile analysis (TPA) using a Texture Analyzer (Model TA, XT Plus, Texture Technologies Corp., United States). After samples were crystallized for 90 min, the crystallized material was placed in a polystyrene assay tube and left at 5 °C for 48 h to allow complete crystallization. Just before performing the TPA analysis, samples were taken out of the assay tube and cut to a 3/4 in height for TPA analysis.[28]

Rheology Measurements. A TA Instruments AR-G2Magnetic Bearing Rheometer (TA Instruments, AR-G2) was used to evaluate the viscoelastic properties of the material. The flow procedure was performed by steady state flow step to evaluate samples' zero-rate viscosity. Oscillatory tests were performed by strain sweep step to obtain viscoelastic parameters such as the storage (G') and loss (G'') modulus.

Table 2. TAG Chemical Composition of the IESBO Expressed as the ECN[a]

ECN	%
38	0.16 ± 0.04
40	2.10 ± 0.03
42	8.25 ± 0.12
44	14.86 ± 1.54
46	24.77 ± 0.56
48	49.86 ± 2.23

[a] ECN = CN − 2*n*, where CN is the total carbon number of the TAG and *n* is the total number of unsaturations.

The experiments were carried out using a parallel plate geometry (40 mm diameter). For a steady state flow step, the shear rate (1/s) was controlled from 1.000×10^{-4} to 100.0; for the strain sweep step, a constant frequency of 1 Hz (6.28 rad/s) was used, and strain values were set from 0.0008 to 10%. The viscoelastic behavior of the samples was measured after 90 min of crystallization and after tempering the material at 5 and 25 °C for 48 h. Different tempering conditions were tested to evaluate how these affect the viscoelastic properties of the material and, therefore, its functional properties.

X-ray Diffraction measurement (XRD). The polymorphic form of the IESBO crystallized at 32 °C with and without the application of HIU was evaluated using XRD Philips X'Pert 3040 MPD (PANalytical, Almelo, The Netherlands) diffractometer system with a single PW3050/00 (θ/2-θ) goniometer. The X-ray source was Cu Kα radiation with a PW3123/00 Monochromator detector system. The software controlling the system is X'Pert Data Collector (v2.0e) (PANalytical, Almelo, The Netherlands). Samples were crystallized as previously described and tempered for 48 h at 25 and 5 °C before XRD determination.

Statistical Analysis. Samples were run in triplicate, and data reported are mean values and standard deviations. Significant differences ($P < 0.05$) were evaluated using a two-way analysis of variance by the GraphPad Prism software, version 4.00 for Windows (GraphPad Software, San Diego, CA).

RESULTS AND DISCUSSION

The TAG chemical composition of the IESBO sample is shown in Table 2. The chemical composition was expressed as percentage of ECN, where ECN = CN − 2*n*; CN is the TAG carbon number, and *n* is the number of unsaturations. The IESBO sample was composed of approximately 50% of TAG of 48 ECN. The entities integrated in this group include OOO, SOL, and SSLn, where O refers to oleic acid, S refers to stearic acid, L refers to linoleic acid, and Ln refers to linolenic acid. The second most abundant group was TAG with 46 ECN, which include OOL, POL, and SLL with a total of approximately 25%. TAGs with 44 ECN constituted approximately 15% of the sample and represent TAGs such as OLL and PLL. Approximately 8% of the sample was composed of TAGs with ECN of 42, which include TAG entities such as LLL and OLLn. Finally, approximately 2.2% of the sample was composed of TAGs with lower ECN (38 and 40), which represented TAGs such as LnLnL and LLLn, respectively.

Table 3 presents the FAME composition of the IESBO. The major component of this shortening was linoleic acid (C18:2) with approximately 42% of the total fat. The second major component was stearic acid (C18:0) with approximately 22%, and the third major component was oleic acid (C18:1) with approximately 17% of the total fat. Palmitic acid (C16:0) constituted only 11% of the total fatty acid content. The total amount of saturated fat in this shortening was approximately 34%.

Table 3. FAME Composition of the IESBO

fatty acid	percentage
C14:0	0.08 ± 0.00
C16:0	10.58 ± 0.01
C16:1	0.08 ± 0.00
C18:0	21.59 ± 0.24
C18:1	17.32 ± 0.01
C18:2	41.55 ± 0.15
C18:3	6.55 ± 0.04
C20:0	0.39 ± 0.00
C20:1	0.17 ± 0.00
C20:2	0.03 ± 0.00
C20:3	0.02 ± 0.00
C22:0	1.51 ± 0.05
C22:4	0.02 ± 0.00
C24:0	0.09 ± 0.01
total	100

As described in the Materials and Methods, lipid samples were crystallized without and with different acoustic power levels at different crystallization temperatures. The melting point of the IESBO sample was 33.4 ± 0.5 °C; therefore, the crystallization temperatures (T_c) chosen in these experiments were 26, 28, 30, and 32 °C.

Figure 1 shows the morphology of IESBO crystals formed at initial steps of crystallization for 26, 28, 30, and 32 °C, with different acoustic power levels when HIU was applied at 10 min. Pictures shown in Figure 1 for samples crystallized at 26−30 °C were taken at 15 min after the sample was placed in the crystallization cell, while pictures shown for the sample crystallized at 32 °C were taken at 20 min. As expected, Figure 1 shows that when samples were crystallized without HIU, the amount of crystals decreased as T_c increased due to a decrease in the driving force (supercooling) for crystallization. In addition, crystallization at lower T_c generated smaller crystals. Figure 1 also shows an evident induction in the crystallization and the generation of smaller crystals as a consequence of HIU application. Higher power levels had a greater effect on crystallization behavior by inducing crystallization and by generating more and smaller crystals. This behavior was observed for all T_c tested. For all T_c, samples reached crystallization temperature at 10 min after the sample was placed in the crystallization cell. Samples crystallized at 26 and 28 °C started to crystallize before the sample reached crystallization temperature, while samples crystallized at 30 and 32 °C started to crystallize at 13 and 20 min, respectively. Because HIU was applied 10 min after the sample was placed in the crystallization cell, some crystals or nuclei were already present in the media when HIU was applied for samples crystallized at 26 and 28 °C. On the other hand, when samples were crystallized at 30 and 32 °C and HIU was applied at 10 min, no crystals were present during sonication. This suggests that HIU induces crystallization in samples crystallized at 30 and 32 °C by inducing primary nucleation in the system.

Figure 2 shows the microstructure of crystals after 90 min at different crystallization temperatures with different HIU power level applications. The effect of HIU in inducing crystallization was maintained during the 90 min of the experiments as shown in Figure 2 where smaller and more crystals are observed still after 90 min at T_c. This effect was more significant when higher

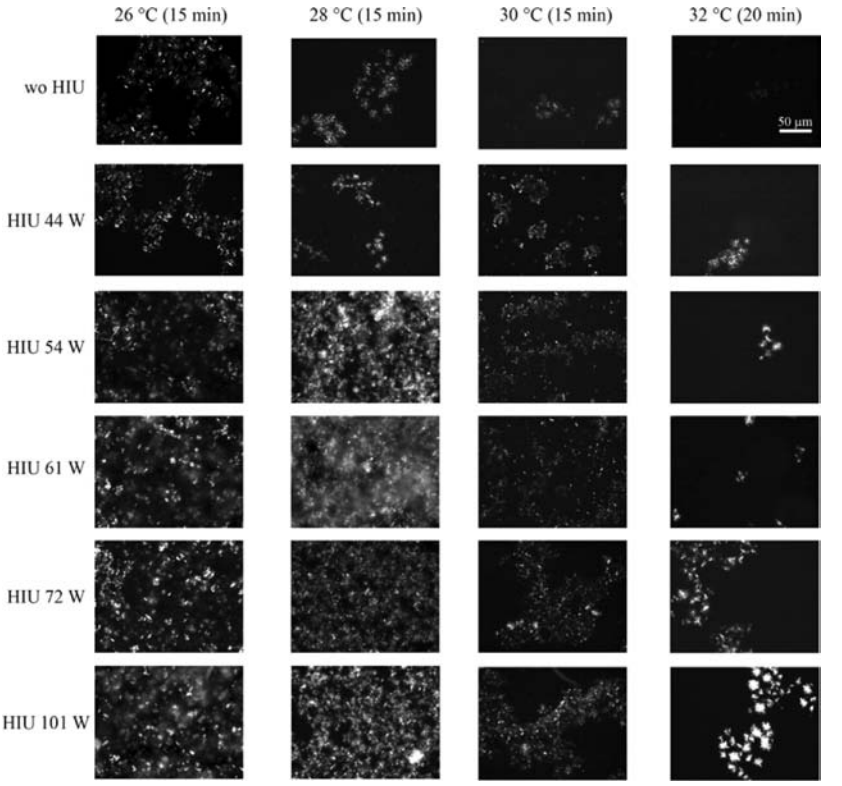

Figure 1. Microstructure of initial lipid crystals obtained when samples were crystallized at 26, 28, 30, and 32 °C without HIU and when HIU was applied at 10 min with different HIU powers (HIU with acoustic power 101, 72, 61, 54, and 44 W). Pictures were taken at 15 min for samples crystallized at 26, 28, and 30 °C and at 20 min for samples crystallized at 32 °C.

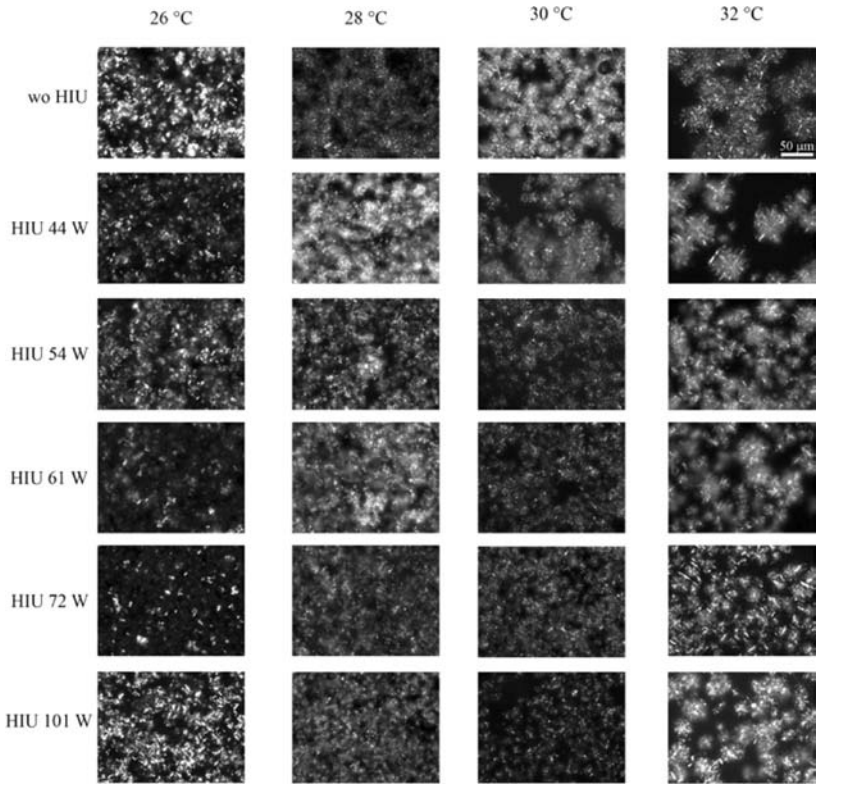

Figure 2. Microstructure of lipid crystals obtained after 90 min at crystallization temperature when samples were crystallized at 26, 28, 30, and 32 °C without HIU and when HIU was applied at 10 min with different HIU powers (HIU with acoustic power 101, 72, 61, 54, and 44 W).

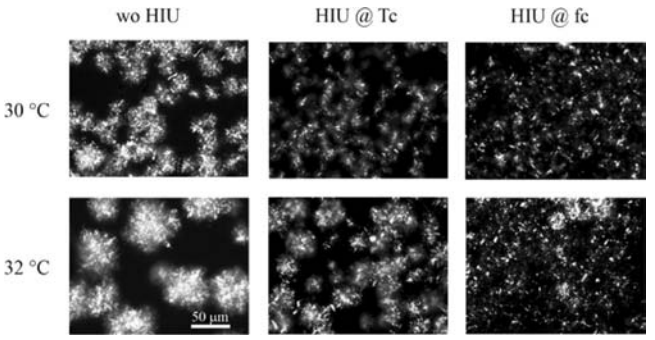

Figure 3. Microstructure of crystals obtained after 90 min of crystallization, HIU (101 W) applied at different moments: T_c indicates that HIU was applied at the moment when the sample reaches crystallization temperature; f_c indicates that HIU was applied at the moment when the first crystals were observed. Agitation was stopped at T_c (10 min), and HIU was applied at f_c (for 30 °C, f_c = 13 min; for 32 °C, f_c = 20 min).

crystallization temperatures were used (T_c = 30 and 32 °C). These results suggest that HIU also affects crystal growth in the system.

It is apparent from the results shown in Figures 1 and 2 that the higher the acoustic power level, the greater the effect that ultrasound played on samples' crystallization behavior, especially on induction of crystallization and crystal size reduction. On the basis of these results, the highest acoustic power (101 W) was used to further evaluate the effect of HIU on the crystallization behavior and functional properties of IESBO. Data discussed above suggest that HIU induces crystallization by promoting primary nucleation when samples are crystallized at high temperatures (30 and 32 °C). When the sample is crystallized at lower temperatures (26 and 28 °C) and HIU is applied in the presence of crystals, HIU might have an effect on secondary nucleation by breaking up the growing crystals and creating more nuclei in the media. This might be a consequence of the high shear forces generated through the sonication. Therefore, additional processing conditions were tested to explore the effect of HIU on lipid crystallization when sonication is applied in the presence or absence of crystals at different T_c. The new processing conditions consisted of (a) applying HIU when sample reached crystallization temperature (T_c) and no crystals are observed and (b) when the first crystals were observed (f_c). For samples crystallized at 32 °C, T_c was reached at 10 min, and the first crystals were observed at approximately 20 min. Therefore, HIU was applied at 10 min (when the sample reached T_c) and at 20 min (when the first crystals were observed). When samples were crystallized at 30 °C, T_c was reached at 10 min, and the first crystals were observed at 13 min. Therefore, HIU was applied at 10 min (sample reached T_c) and at 13 min (when first crystals were observed). In this case, the T_c condition is too close in time to f_c conditions; therefore, a third condition was used for this sample to evaluate the effect of HIU before crystallization occurs and also at a time significantly distant from the moment at which crystallization occurs. To achieve this goal, the third processing condition consisted of stopping agitation at 5 min and immediately applying HIU. When agitation was stopped at 5 min, crystallization started at approximately 10 min. This last condition was also used for samples crystallized at 28 and 26 °C. The nomenclature used to identify these processing conditions is summarized in Table 1.

Figure 3 compares the microstructure obtained after 90 min into the crystallization process when samples were crystallized at

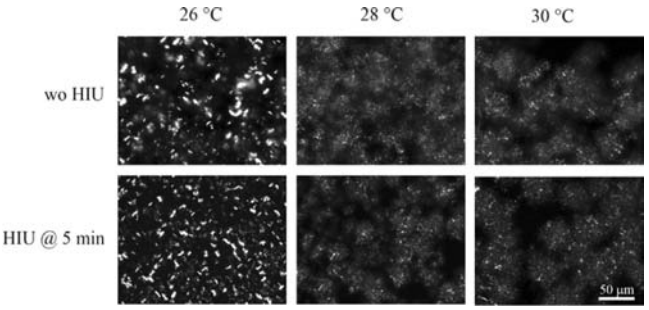

Figure 4. Microstructure of crystals obtained after 90 min of crystallization: Agitation was stopped at 5 min, and HIU (101 W) was applied at 5 min.

30 and 32 °C and HIU was applied at T_c and f_c. The T_c condition always corresponds to HIU being applied at 10 min into the crystallization process, while f_c corresponds to HIU being applied at 13 min for samples crystallized at 30 °C (10/13 in Table 1) and 20 min for samples crystallized at 32 °C (10/20 in Table 1). Micrographs presented in this figure show that HIU is more efficient in reducing crystal size when it is applied using the f_c condition; that is, when HIU is applied in the presence of crystals. These results suggest that the effect of HIU on secondary nucleation is more significant than the one observed for primary nucleation. The crystal size reduction observed when T_c condition is used (no crystals observed) suggests that primary nucleation is affected by acoustic waves, while the crystal size reduction observed when the f_c condition is used suggests that HIU affects secondary nucleation events. The effect of HIU on the morphology of the crystals is maintained even after 90 min of processing, suggesting that crystal growth also might be affected.

Figure 4 shows the microstructure of crystals obtained after 90 min into the crystallization process when agitation was stopped at 5 min and HIU immediately applied for sample crystallized at 26, 28, and 30 °C. When samples were crystallized without the use of HIU, the induction times of crystallization were 12, 14, and 15 min for samples crystallized at 26, 28, and 30 °C, respectively. It is evident from these pictures that a reduction in crystal size is obtained as a consequence of HIU application, especially when samples are crystallized at low T_c (26 °C). However, as previously discussed, this is a less effective way to reduce the size of crystals than when HIU is applied when crystals are present in the medium (Figure 2).

Previous research[16] on sonocrystallization in aqueous systems suggests that the induction in crystallization caused by acoustic waves is due to several factors: (a) the generation of cavitation and (b) shear forces caused by the acoustic waves. Data described above suggest that in lipid systems HIU is more effective when applied in the presence of crystals. This increased effect observed with the presence of crystals can be explained by a combining effect of cavitation and shear forces caused by the acoustic waves. In the presence of crystals, shear forces might break some of the existing crystals, creating new nuclei and resulting in the generation of more and smaller crystals in the network. Similarly, when no crystals are present and HIU is applied, only cavitation events are responsible for inducing crystallization. That is, small bubbles generated during the sonication act as nuclei inducing crystallization in the system.

In general, lipid crystal networks with small crystal sizes result in harder materials.[27,28] Therefore, we expect that this crystal size reduction caused by HIU will generate harder materials in terms

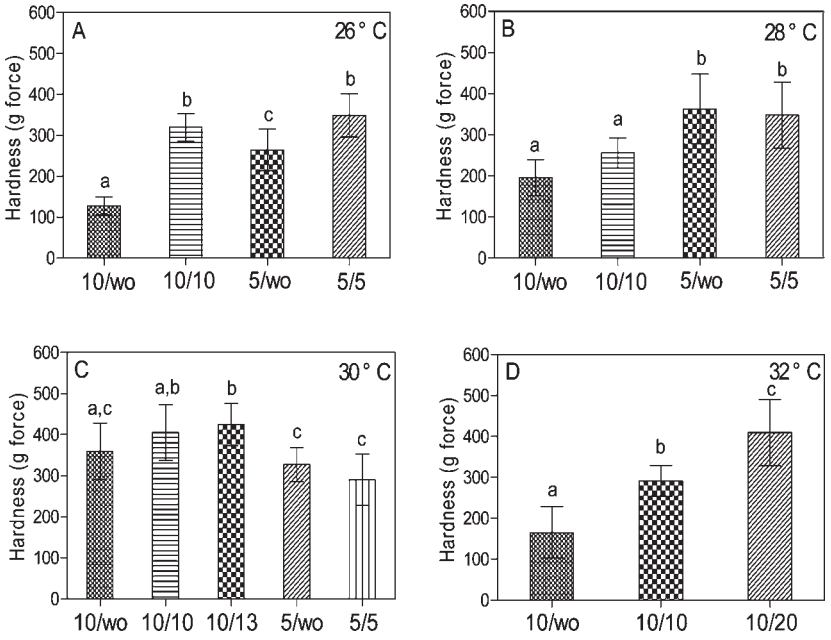

Figure 5. Hardness (expressed in gram force) of the samples determined by TPA; samples crystallized at 26 (A), 28 (B), 30 (C), and 32 °C (D) were stored for 48 h at 5 °C.

of texture and viscoelastic properties. Figure 5 shows the hardness of samples crystallized at different temperatures without and with the application of HIU when samples were crystallized under the conditions described previously. As described in the Materials and Methods, hardness was measured with TPA after tempering the crystallized sample for 48 h at 5 °C to allow complete crystallization and the formation of stable structures. Hardness of samples crystallized without HIU application, for which agitation was stopped at 5 min (5/wo), was higher (26 and 28 °C) or equal (30 °C) than samples where agitation was stopped at 10 min (10/wo). For samples crystallized at 26 °C, HIU always generated a significantly harder material ($p < 0.05$). Interestingly, the same behavior was not observed for samples crystallized at 28 and 30 °C where even though HIU generated harder materials when agitation was stopped at 10 min, the differences were not statistically significant. When samples were crystallized at 32 °C, the hardness of sonicated samples was significantly higher ($p < 0.05$) for all conditions tested, and the harder texture was observed for samples where HIU was applied under f_c conditions (10/20). This finding is in accordance to the microstructure observed and reported in Figure 3 where significantly smaller crystals were observed for the f_c condition. The texture observed in these measurements is driven by the microstructure of the crystal network formed where smaller crystals are usually associated with harder materials. Crystals formed during the crystallization experiments for 90 min and crystals formed during the tempering at 5 °C are responsible for these textural properties. Micrographs reported in this study show that HIU induces crystallization in the samples; however, the long-term effect of sonication during tempering at lower temperatures is unknown. That is, for samples crystallized at intermediate temperatures (28 and 30 °C), crystallization might continue during the tempering step; therefore, bigger crystals are obtained without showing the consequent increase in sample texture. For low crystallization temperatures, 26 °C, the high supercooling and HIU application resulted in very fast crystallization during the first 90 min, allowing samples to reach equilibrium during this time. Therefore, no additional crystallization occurs during storage at 5 °C and differences in microstructure and therefore texture are observed after 48 h of storage at 5 °C. Similarly, when samples were crystallized at high temperatures, 32 °C, HIU induced crystallization, but the low supercooling in the system did not allow for further crystallization to occur. When the samples are stored at lower temperatures, the liquid material in the sample crystallizes rapidly, forming several small crystals. These combined effects result in a harder crystal network.

The thermal behavior of the crystallized material after 90 min at T_c and after tempering for 48 h at 5 °C was evaluated using DSC, as described in the Materials and Methods. Figure 6 shows the melting profile of the samples crystallized at different crystallization temperatures with and without HIU application after 90 min (Figure 6A–D) into the crystallization process and after tempering for 48 h at 5 °C (Figure 6E,F). Figure 6A–D shows a single melting peak characterized by a peak temperature of 43.2 ± 1.5 °C. When samples were crystallized with HIU, the melting peaks became broader with an evident shoulder at lower temperatures. This is more evident for samples that were crystallized with HIU under the f_c condition. These findings suggest that HIU might induce a slight fractionation of the crystals network. As expected, after tempering the samples at 5 °C for 48 h, two melting peaks were observed (Figure 6E–H). The first melting peak on the left shows the secondary crystallization after tempering with a melting temperature of 19.4 ± 1.6 °C. The second melting peak represents crystals formed during the 90 min crystallization process and the recrystallization or crystal growth during tempering with a melting temperature of 43.3 ± 2.1 °C. The fractionation described for the melting profiles observed after 90 min at T_c (Figure 6A–D) is still observed after tempering. Melting enthalpies calculated from the endotherm observed after 90 min into the crystallization process values were not significantly different among samples crystallized with and without HIU application. Enthalpy values for samples

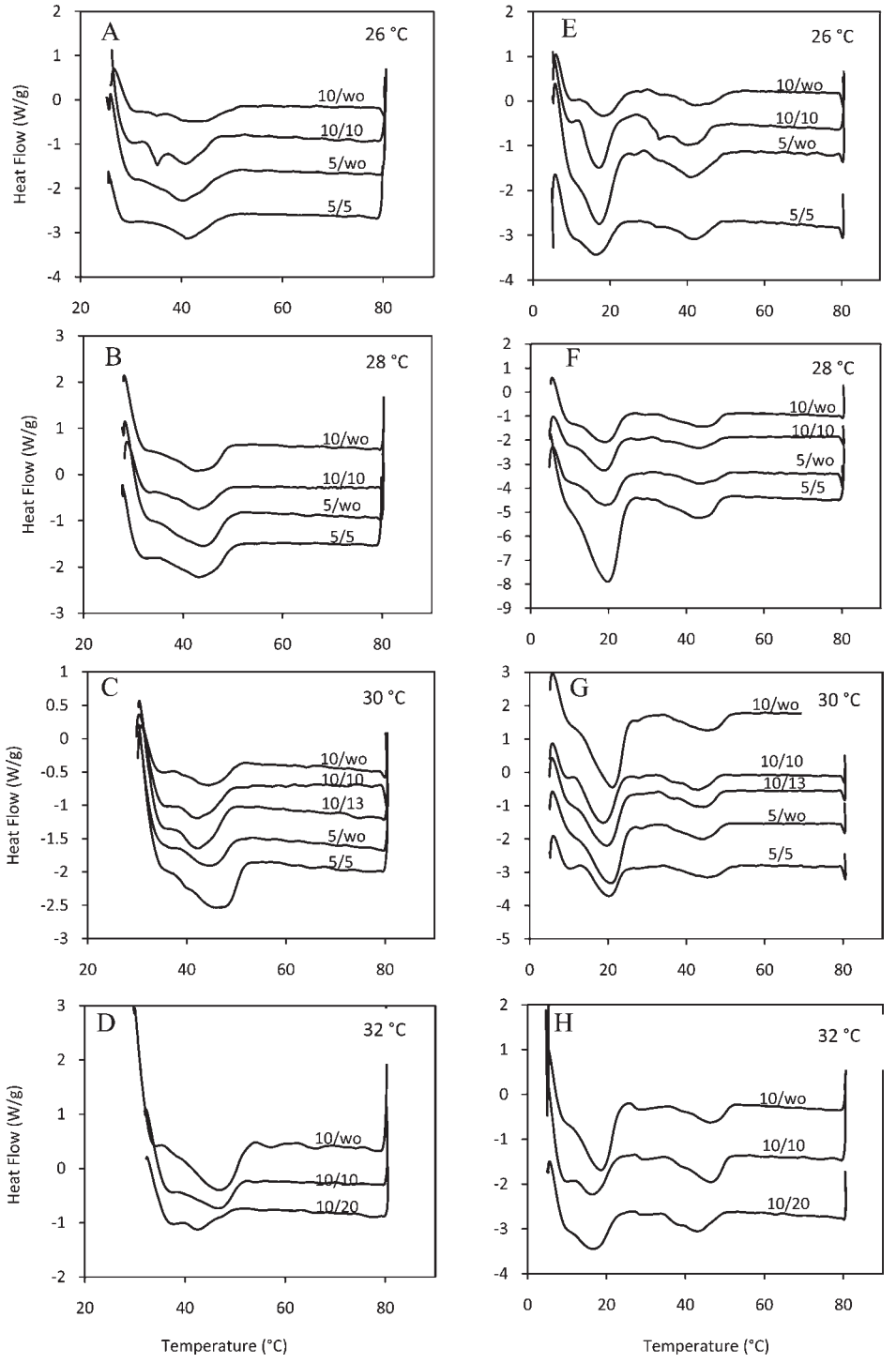

Figure 6. DSC melting profiles of the samples crystallized at different crystallization temperatures with and without HIU application after 90 min (A–D) into the crystallization process and after tempering for 48 h at 5 °C (E–H).

crystallized at 26 °C without HIU and with HIU (10/10) were 4.39 ± 0.64 and 4.36 ± 0.42 J/g. Similar results were obtained for samples crystallized at 28 °C with enthalpy values of 4.19 ± 0.60 and 4.62 ± 1.41 J/g for samples crystallized with HIU (10/10) and without HIU, respectively. Enthalpy values for samples crystallized at 30 °C were slightly lower with values of 3.78 ± 1.13, 4.81 ± 1.44, and 3.35 ± 0.45 J/g for samples crystallized without HIU, with HIU (10/10), and with HIU (10/13). When samples were crystallized at 32 °C, enthalpy values were 4.35 ± 0.95, 5.56 ± 1.18, and 5.76 ± 0.88 J/g for samples crystallized without HIU and with HIU applied at 10 (10/10) and 20 min (10/20), respectively. Enthalpy values were also calculated after samples were tempered for 48 h at 5 °C. The second endotherm was used to calculate this parameter. As previously described, no significant differences were found for the enthalpy values among samples with and without HIU application. Enthalpy values for

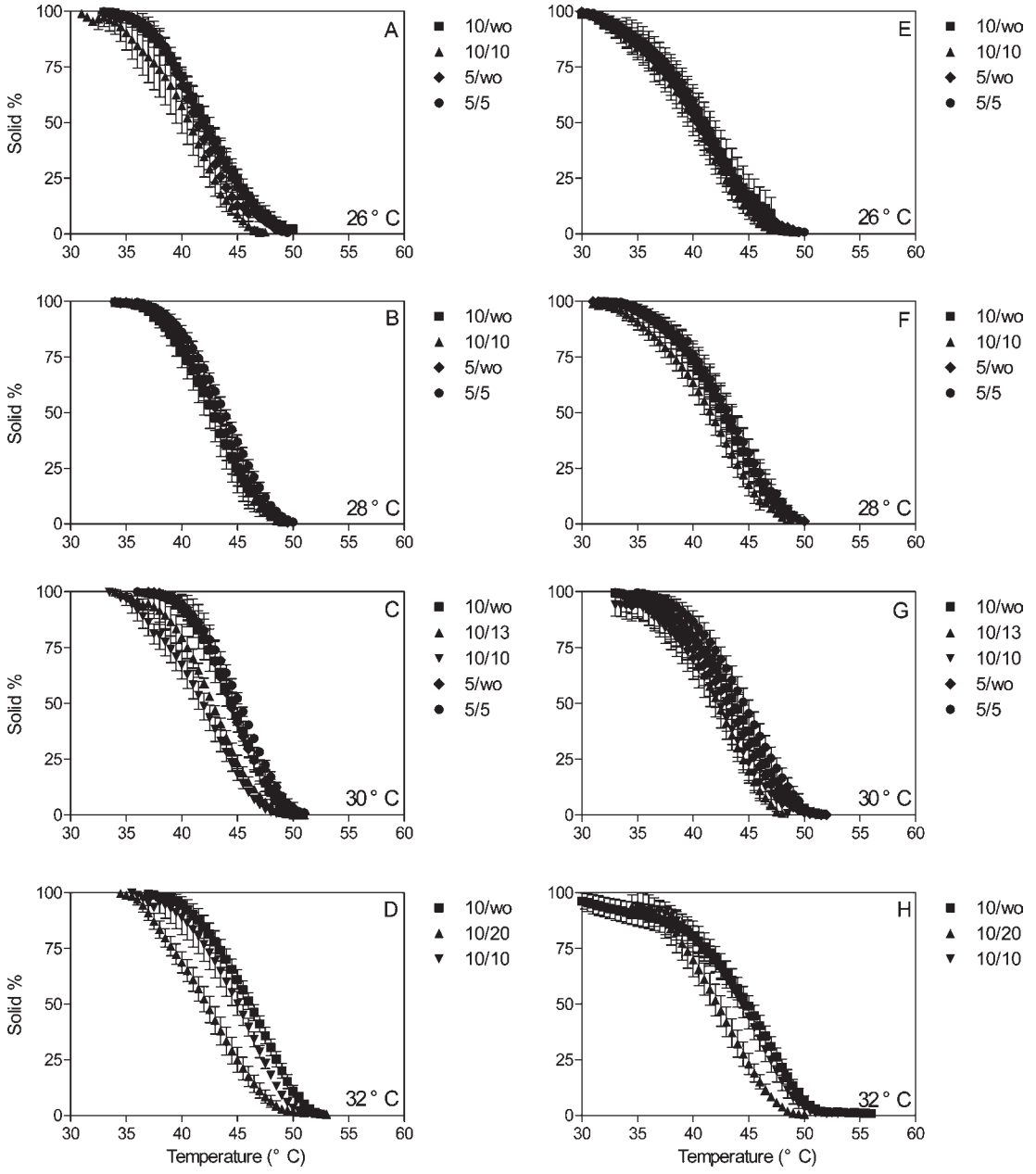

Figure 7. Percentage of remaining solid material as a function of temperature for samples crystallized at different conditions after 90 min (A−D) and after tempering for 48 h at 5 °C (E−H).

samples crystallized at 26 °C were 6.96 ± 0.61 and 7.19 ± 1.28 J/g for samples crystallized without HIU and with HIU, respectively. Enthalpy values for samples crystallized at 28 °C were 6.64 ± 0.89 and 7.39 ± 0.71 J/g for samples crystallized with HIU and without HIU, respectively. Similarly, enthalpy values for samples crystallized at 30 °C were 6.31 ± 1.34, 6.86 ± 0.47, and 5.84 ± 0.94 J/g for samples crystallized without HIU, with HIU (10/10), and with HIU (10/13). Finally, when samples were crystallized at 32 °C, enthalpy values were 5.66 ± 0.74, 5.71 ± 1.49, and 5.67 ± 0.67 J/g for samples crystallized without HIU and with HIU applied at 10 (10/10) and 20 min (10/20), respectively. These data suggest that further crystallization occurred during the tempering at 5 °C for 48 h as evidenced by the slighter enthalpy values reported. However, no differences were found in the enthalpy values of the samples crystallized with and without HIU in any of the conditions used before and after tempering. These results suggest that the effect of HIU on the crystallization of IESBO is mainly on the generation of smaller crystals but not on the amount of crystallized material.

Figure 7 shows the amount of solids remaining at a specific temperature (% solid) as the sample is being heated in the DSC. This figure aids in the quantification of the melting profile of crystals formed during crystallization. Figure 7A−D shows the % solid for the crystal network formed after 90 min at T_c, while Figure 7E−H shows the % solid for the crystal network formed after tempering for 48 h at 5 °C. Samples crystallized at 30 and 32 °C with HIU had a steeper melting profile. This effect is more evident for the f_c conditions (10/13 and 10/20), while the effect seems to be lost after tempering for 48 h at 5 °C for the samples crystallized at 30 °C (Figure 7G), and it is still present for the

Table 4. Viscoelastic Parameters (G' and G'') of IESBO Crystallized at Different Temperatures (26, 28, 30, and 32 °C) for 90 min[a]

	26 °C		28 °C		30 °C		32 °C	
	G' (Pa)	G'' (Pa)	G' (Pa)	G'' (Pa)	G' (Pa)	G'' (Pa)	G' (Pa)	G'' (Pa)
10/wo	391.5 ± 27.0 a	48.8 ± 4.9 a	470.9 ± 307.0 a,b	47.5 ± 19.5 a	2610.0 ± 83.4 a	148.3 ± 2.5 a	194.9 ± 17.9 a	20.1 ± 3.5 a
10/10	1839.0 ± 684.5 b	176.6 ± 23.1 b	1564.0 ± 19.8 b,c	154.3 ± 2.6 b	1410.5 ± 152.0 b	91.6 ± 10.2 b	597.2 ± 159.6 a	60.3 ± 15.7 a
10/13	N/A	N/A	N/A	N/A	2793.5 ± 53.0 a	185.8 ± 20.0 a	N/A	N/A
10/20	N/A	N/A	N/A	N/A	N/A	N/A	4229.0 ± 1277.0 b	160.0 ± 5.6 b
5/wo	248.7 ± 82.7 a	31.9 ± 3.8 a	1809.5 ± 413.6 c	125.0 ± 22.5 b	295.2 ± 48.0 c	29.1 ± 2.9 c	N/A	N/A
5/5	315.1 ± 55.6 a	36.5 ± 5.3 a	535.9 ± 129.4 b	50.0 ± 1.9 a	146.5 ± 123.3 c	17.4 ± 9.3 c	N/A	N/A

[a] N/A, not applicable. The table shows mean values and standard deviations. Letters with the same letter within a column indicates that values are not significantly different ($\alpha = 0.05$).

Table 5. Viscoelastic Parameters (G' and G'') of IESBO Crystallized at Different Temperatures (26, 28, 30, and 32 °C) for 90 min and Tempered at 5 °C for 48 h[a]

	26 °C		28 °C		30 °C		32 °C	
	G' ($\times 10^5$ Pa)	G'' ($\times 10^5$ Pa)	G' ($\times 10^5$ Pa)	G'' ($\times 10^5$ Pa)	G' ($\times 10^5$ Pa)	G'' ($\times 10^5$ Pa)	G' ($\times 10^5$ Pa)	G'' ($\times 10^5$ Pa)
10/wo	2.6 ± 2.5 a,c	0.5 ± 0.3 a	9.0 ± 0.3 a,b	1.3 ± 0.6 a	5.9 ± 0.8 a	0.9 ± 0.1 a	1.2 ± 0.5 a	0.24 ± 0.01 a
10/10	11.5 ± 0.2 b	1.84 ± 0.03 b	10.8 ± 1.0 a	1.8 ± 0.1 a	8.9 ± 0.6 a	1.4 ± 0.1 a	7.8 ± 0.4 b	1.1 ± 0.1 b
10/13	N/A	N/A	N/A	N/A	7.0 ± 2.0 a	1.2 ± 0.4 a	N/A	N/A
10/20	N/A	N/A	N/A	N/A	N/A	N/A	9.7 ± 0.3 c	1.7 ± 0.1 c
5/wo	7.4 ± 1.1 b,c	0.7 ± 0.1 a	6.0 ± 1.1 b	0.9 ± 0.3 a	5.0 ± 0.3 a	0.7 ± 0.1 a	N/A	N/A
5/5	4.8 ± 0.5 c	0.7 ± 0.1 a	11.59 ± 0.01 a	2.2 ± 0.7 a	12.8 ± 5.3 a	1.7 ± 0.6 a	N/A	N/A

[a] N/A, not applicable. The table shows mean values and standard deviations. Letters with the same letter within a column indicates that values are not significantly different ($\alpha = 0.05$).

sample crystallized at 32 °C (Figure 7H). Similar results were reported by Suzuki et al.[28] in other lipid systems such as anhydrous milk fat and an all-purpose shortening. The steeper melting profiles observed as a consequence of HIU can be a result of the smaller crystals formed during sonication, and therefore a faster melting rate, or to the fractionation reported in Figure 6.

Tables 4−7 show the viscoelastic properties of samples crystallized with and without HIU application after 90 min into the crystallization process and after tempering for 48 h at 25 and 5 °C. In general, higher storage modulus (G') values were obtained when agitation was stopped at 10 min, and samples were crystallized with HIU, especially when acoustic waves were applied when the first crystals were observed. Similar tendencies to the ones observed for G' were observed for the loss modulus (G'') values. Table 4 shows the storage (G') and loss modulus (G'') values for samples crystallized at different temperatures with and without the use of HIU of the crystal network formed after 90 min at T_c. When HIU was applied at 10 min (10/10) and samples were crystallized at 26, 28, and 32 °C, both G' and G'' increase consistently with a larger increase in G' as compared to that observed for G''. The biggest differences in G' were observed for samples crystallized at 26 and 32 °C in accordance with the previously discussed TPA data, where smaller differences in hardness were observed for samples crystallized at 28 and 30 °C (Figure 5). At 26 °C, G' increases from 391.5 to 1839 Pa, while G'' increases from 48.8 Pa to 176.7. When HIU was applied at 20 min at 32 °C, the most significant increase in G' and G'' was observed. Values of G' increased from 195 to 4229 Pa, with more than 20 times increase, and G'' increases seven times from 20 to 160 Pa. The value of G' for HIU applied at 20 min is significantly larger than that for HIU applied at 10 min ($P < 0.05$); these data also support the hypothesis that HIU is more effective when it is applied in the presence of crystals.

Table 5 shows the variations of G' and G'' of samples with and without HIU application after tempering the samples for 48 h at 5 °C. Tempering samples for 48 h at 5 °C increases G' values significantly as compared to the values obtained after 90 min into the crystallization process. This is an expected result since crystallization of low melting TAGs occurs at this lower temperature; therefore, harder materials are expected. As described for data presented in Table 4, G' and G'' values were higher when samples were crystallized with HIU, especially when 26 and 32 °C were used as crystallization temperatures. Interestingly, during tempering at 5 °C, samples crystallized at 30 °C with HIU application showed slightly higher elastic properties (higher G') than the sample crystallized at the same temperature but without HIU. These data are in accordance with the hardness values discussed in Figure 5 and suggest that different recrystallization mechanisms occur during the tempering process when HIU is applied at this T_c.

Shortening producers use different tempering profiles before the product reaches the consumer. Therefore, a second tempering procedure was tested to evaluate the effect of sonication on the viscoelastic properties of the material. Table 6 shows viscoelastic parameters (G' and G'') for samples tempered for 48 h at 25 °C. In general, G' and G'' values were lower than the ones reported in Tables 4 and 5, suggesting that crystal reorganization occurs during tempering with the generation of less solidlike structures. Nevertheless, significant differences between sonicated and nonsonicated samples still exist. It is interesting to note that the biggest differences were found in samples that were crystallized using HIU with significantly higher values observed

Table 6. Viscoelastic Parameters (G' and G'') of IESBO Crystallized at Different Temperatures (26, 28, 30, and 32 °C) for 90 min and Tempered at 25 °C for 48 h[a]

	26 °C		28 °C		30 °C		32 °C	
	G' (Pa)	G'' (Pa)	G' (Pa)	G'' (Pa)	G' (Pa)	G'' (Pa)	G' (Pa)	G'' (Pa)
10/wo	39.4 ± 2.6 a	15.6 ± 0.9 a	43.6 ± 28.4 a	14.8 ± 3.4 a	57.8 ± 8.3 a	17.1 ± 0.1 a	25.3 ± 10.9 a	9.9 ± 3.0 a
10/10	2595.5 ± 234.0 b	297.1 ± 50.5 b	532.2 ± 83.7 b	109.1 ± 9.0 b	202.6 ± 120.3 a	36.5 ± 10.3 a	254.2 ± 117.3 a	44.5 ± 16.0 a
10/13	N/A	N/A	N/A	N/A	129.4 ± 88.5 a	26.8 ± 13.7 a	N/A	N/A
10/20	N/A	N/A	N/A	N/A	N/A	N/A	1719.5 ± 186 b	263.1 ± 10.0 b
5/wo	61.6 ± 34.5 a	17.5 ± 3.3 a	56.8 ± 14.0 a	17.2 ± 0.1 a	37.0 ± 13.8 a	14.1 ± 3.8 a	N/A	N/A
5/5	117.0 ± 31.0 a	28.5 ± 7.4 a	21.6 ± 3.0 a	11.0 ± 1.1 a	41.9 ± 21.3 a	13.3 ± 3.2 a	N/A	N/A

[a] N/A, not applicable. The table shows mean values and standard deviations. Letters with the same letter within a column indicates that values are not significantly different ($\alpha = 0.05$).

Table 7. Zero-Rate Viscosity Values (Pa s × 10^4) of IESBO Crystallized at Different Temperatures (26, 28, 30, and 32 °C) for 90 min and Tempered at 25 °C for 48 h[a]

	26 °C		28 °C		30 °C		32 °C	
	90 min	48 h at 25 °C	90 min	48 h at 25 °C	90 min	48 h at 25 °C	90 min	48 h at 25 °C
10/wo	0.4 ± 0.1 a	0.12 ± 0.03 a	0.6 ± 0.1 a	3.8 ± 0.9 a	1.6 ± 0.9 a	5.5 ± 0.4 a	0.2 ± 0.1 a	0.3 ± 0.1 a
10/10	2.3 ± 0.3 b	1.8 ± 0.1 b	2.1 ± 0.6 b	1.0 ± 0.1 b	1.21 ± 0.03 a	19.3 ± 3.2 b	0.9 ± 0.2 a	24.0 ± 4.2 b
10/13	N/A	N/A	N/A	N/A	13.4 ± 4.6 b	6.9 ± 2.0 a	N/A	N/A
10/20	N/A	N/A	N/A	N/A	N/A	N/A	4.0 ± 0.2 b	5.4 ± 0.6 a
5/wo	0.4 ± 0.1 a	0.4 ± 0.1 a	5.26 ± 0.05 a	0.3 ± 0.1 b	1.5 ± 0.1 a	0.9 ± 0.2 a	N/A	N/A
5/5	0.71 ± 0.02 a	1.02 ± 0.05 c	0.47 ± 0.04 a	0.7 ± 0.1 b	0.5 ± 0.3 a	5.5 ± 0.4 a	N/A	N/A

[a] N/A, not applicable. The table shows mean values and standard deviations. Letters with the same letter within a column indicates that values are not significantly different ($\alpha = 0.05$).

for samples crystallized at 26, 28, and 32 °C when agitation was stopped at 10 min and HIU was applied in the presence of crystals. No significant differences were found in the samples where agitation was stopped at 5 min in any of the conditions tested. On the basis of these observations, we proposed that HIU might have the function of stabilizing small lipid crystals when stored at room temperature, which is good evidence for industry production of lipid-based food.

Table 7 shows the zero-rate viscosity of samples after 90 min into the crystallization process and after tempering at 25 °C for 48 h. The viscosity of samples tempered at 5 °C was not measured since these were too hard to perform this type of measurement. Viscosity values show tendencies similar to those described for G' and G'', suggesting that HIU application generated crystal networks with higher viscosity. As previously discussed, the effect of HIU in increasing sample viscosity was more significant when samples crystallized at 26, 28, and 32 °C for 90 min and when HIU was applied in the presence of crystals. It is interesting to note that the viscosity of some of the samples increased during tempering at 25 °C for 48 h. In general, samples with high viscosity values after 90 min (samples crystallized with HIU application in the presence of crystals) showed a slight decrease in viscosity with tempering, while those samples with low viscosity values after 90 min showed an increased viscosity after tempering. For example, values of viscosity for samples crystallized without HIU at 28 °C increased after tempering. Similarly, samples crystallized at 32 °C with HIU applied at 10 min increased significantly after tempering as compared to the values after 90 min of crystallization. On the other hand, samples crystallized at 30 °C with HIU applied when the first crystals were observed (10/13) had a significantly lower viscosity after tempering for 48 h at 25 °C. These results suggest that different mechanisms of recrystallization occur during tempering of samples treated with different HIU conditions.

XRD was performed in samples crystallized at 32 °C with and without the use of HIU after 90 min into the crystallization process and after tempering for 48 h at 5 and 25 °C. Only these conditions were tested since they are the ones that show more effect of sonication on the crystallization behavior of the IESBO. In all cases, the XRD patterns were characteristic of the β'-form with two strong signals at 3.8 and 4.3 Å. No signal at 4.6 Å, characteristic of the β-form, was found. This finding suggests that changes observed in this study are not due to different polymorphic forms generated by sonication and/or storage.

In summary, this research shows that HIU can modify the crystallization behavior of a low saturated shortening (IESBO). Specific changes include the induction in the onset of crystallization, the reduction of crystal size, and the generation of harder and more elastic materials. The effectiveness of this novel technology depends on the acoustic power used and on several processing conditions, such as crystallization temperature and application time. HIU induces primary and secondary nucleation and might also promote crystal growth. In addition, results show that HIU is more efficient when it is applied in the presence of crystals or nuclei. These results suggest that HIU can be used as an additional tool to improve the crystal network of lipids with low contents of saturated fatty acids, by modifying the physicochemical characteristics of the material such as texture and viscoelasticity. HIU can not only induce the crystallization and promote the growth of crystals but also has the function of

stabilizing the crystals formed as evidenced in the tempering experiments.

AUTHOR INFORMATION

Corresponding Author

*Tel: 435-797-8136. Fax: 435-797-2179. E-mail: silvana.martini@usu.edu. Website: http://www.MartiniResearch.com.

Funding Sources

Funding was provided by USDA-CSREES (project 2009-65503-05789). This paper was approved by the Utah Agricultural Experiment Station as paper no. 8324.

ACKNOWLEDGMENT

We thank ADM for providing the sample and Dr. Marie Walsh and Dr. Robert Ward for the HPLC and GC analysis of the sample.

REFERENCES

(1) Institute of Shortenings and Vegetable Oils. Domestic shipments of Edible Fats and Oils. 2010; available from http://www.iseo.org/statistics.htm.

(2) Puri, P. S. Correlations for Trans-Isomer Formation during Partial Hydrogenation of Oils and Fats. *J. Am. Oil Chem. Soc.* **1978**, *55*, A263–A263.

(3) Izadifar, M. Neural network modeling of trans isomer formation and unsaturated fatty acid changes during vegetable oil hydrogenation. *J. Food Eng.* **2005**, *66*, 227–232.

(4) Okonek, D. V.; Alcorn, W. R.; Cullo, L. A. Characteristics of Nickel-Sulfur Catalysts in the Hydrogenation of Soybean Oil at Trans Isomer Producing Conditions. *J. Am. Oil Chem. Soc.* **1980**, *57*, A137–A137.

(5) Cizmeci, M.; Musavi, A.; Tekin, A.; Kayahan, M. Catalytic behavior of ruthenium in soybean oil hydrogenation. *Eur. J. Lipid Sci. Technol.* **2009**, *111*, 607–611.

(6) Cizmeci, M.; Musavi, A.; Kayahan, M.; Tekin, A. Monitoring of hydrogenation with various catalyst ratios. *J. Am. Oil Chem. Soc.* **2005**, *82*, 925–929.

(7) Musavi, A.; Cizmeci, M.; Tekin, A.; Kayahan, M. Effects of hydrogenation parameters on trans isomer formation, selectivity and melting properties of fat. *Eur. J. Lipid Sci. Technol.* **2008**, *110*, 254–260.

(8) Valenzuela, A.; King, J.; Nieto, S. Trans fatty acid isomers from hydrogenated fats: The controversy about health implications. *Grasas Aceites* **1995**, *46*, 369–375.

(9) Nasirullah; Shariff, R.; Shetty, U. S.; Yella, R. S. Development of chemically interesterified healthy coconut oil blends. *Int. J. Food Sci. Technol.* **2010**, *45*, 1395–1402.

(10) Dogan, I. S.; Javidipour, I.; Akan, T. Effects of interesterified palm and cottonseed oil blends on cake quality. *Int. J. Food Sci. Technol.* **2007**, *42*, 157–164.

(11) Javidipour, I.; Tuncturk, Y. Effect of using interesterified and non-interesterified corn and palm oil blends on quality and fatty acid composition of Turkish White cheese. *Int. J. Food Sci. Technol.* **2007**, *42*, 1465–1474.

(12) Nagaraju, A.; Lokesh, B. R. Interesterified coconut oil blends with groundnut oil or olive oil exhibit greater hypocholesterolemic effects compared with their respective physical blends in rats. *Nutr. Res. (N.Y.)* **2007**, *27*, 580–586.

(13) Ozvural, E. B.; Vural, H. Utilization of interesterified oil blends in the production of frankfurters. *Meat Sci.* **2008**, *78*, 211–216.

(14) Martini, S.; Award, T.; Marangoni, A. Structure and properties of fat crystal networks. In *Modifying Lipids for Use in Food*; Gunstone, F., Ed.; CRC: New York, 2006; pp 142−169.

(15) Narine, S. S.; Marangoni, A. G. Microstructure. In *Fat Crystal Networks*; Marangoni, A. G., Ed.; Marcel Dekker: New York, 2005; pp 179−254.

(16) Patist, A.; Bates, D. Ultrasonic innovations in the food industry: From the laboratory to commercial production. *Innovative Food Sci. Emerging Technol.* **2008**, *9*, 147–154.

(17) Chow, R.; Blindt, R.; Chivers, R.; Povey, M. The sonocrystallisation of ice in sucrose solutions: primary and secondary nucleation. *Ultrasonics* **2003**, *41*, 595–604.

(18) Chow, R.; Blindt, R.; Chivers, R.; Povey, M. A study on the primary and secondary nucleation of ice by power ultrasound. *Ultrasonics* **2005**, *43*, 227–30.

(19) Patel, S. R.; Murthy, Z. V. P. Ultrasound assisted crystallization for the recovery of lactose in an anti-solvent acetone. *Cryst. Res. Technol.* **2009**, *44*, 889–896.

(20) McCausland, L. J. Production of crystalline materials by using high intensity ultrasound. U.S. Patent 7244307 10/513154, 2007.

(21) Luque de Castro, M. D.; Priego-Capote, F. Ultrasound-assisted crystallization (sonocrystallization). *Ultrason. Sonochem.* **2007**, *14*, 717–24.

(22) Virone, C.; Kramer, H. J. M.; van Rosmalen, G. M.; Stoop, A. H.; Bakker, T. W. Primary nucleation induced by ultrasonic cavitation. *J. Cryst. Growth* **2006**, *294*, 9–15.

(23) Kallies, B.; Ulrich, J.; König, A. Production of Crystal Suspensions for Granulation Processes. *Trans. IChemE* **1997**, *75* (Part A 2), 142–146.

(24) Ueno, S.; Sakata, J.; Takeuchi, M.; Sato, K. Study for ultrasonic stimulation effect on promotion of crystallization of triacylglycerols. *Photon Factory Activity Report*, 2002; p 182.

(25) Ueno, S.; Ristic, R.; Higaki, K.; Sato, K. In situ studies of ultrasound-stimulated fat crystallization using synchrotron radiation. *J. Phys. Chem. B* **2003**, *107*, 4927–4935.

(26) Ueno, S.; Minato, A.; Seto, H.; Amemiya, Y.; Sato, K. Synchrotron radiation X-ray diffraction study of liquid crystal formation and polymorphic crystallization of SOS (sn-1,3-distearoyl-2-oleoyl glycerol. *J. Phys. Chem. B* **1997**, *101*, 6847–6854.

(27) Martini, S.; Suzuki, A. H.; Hartel, R. W. Effect of high intensity ultrasound on crystallization behavior of anhydrous milk fat. *J. Am. Oil Chem. Soc.* **2008**, *85*, 621–628.

(28) Suzuki, A. H.; Lee, J.; Padilla, S. G.; Martini, S. Altering functional properties of fats using power ultrasound. *J. Food Sci.* **2010**, *75*, E208–14.

(29) O'Fallon, J. V.; Busboom, J. R.; Nelson, M. L.; Gaskins, C. T. A direct method for fatty acid methyl ester synthesis: Application to wet meat tissues, oils, and feedstuffs. *J. Anim. Sci.* **2007**, *85*, 1511–1521.